# Thermal IR Detection With Nanoelectromechanical Silicon Nitride Trampoline Resonators

Markus Piller, Johannes Hiesberger, Elisabeth Wistrela, Paolo Martini, Niklas Luhmann, and Silvan Schmid

***Abstract*—Nanoelectromechanical (NEMS) resonators are promising uncooled thermal infrared (IR) detectors to overcome existing sensitivity limits. Here, we investigated NEMS trampoline resonators made of silicon nitride (SiN) as thermal IR detectors. Trampolines have an enhanced responsivity of more than two orders of magnitude compared to state-of-the-art SiN drums. The characterized NEMS trampoline IR detectors yield a sensitivity in terms of noise equivalent power (NEP) of 7 pW/$\sqrt{\text{Hz}}$ and a thermal response time as low as 4 ms. The detector area features an impedance-matched metal thin-film absorber with a spectrally flat absorption of 50% over the entire mid-IR spectral range from 1 to 25 $\mu$m.**

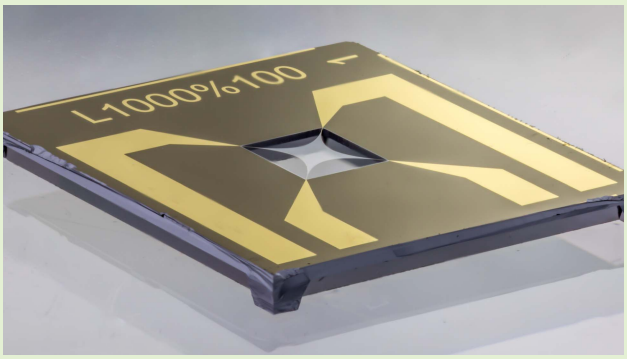

***Index Terms*— Low-pressure chemical vapor deposition (LPCVD) silicon nitride (SiN), nanoelectromechanical (NEMS), thermal infrared (IR) detector, trampoline resonator.**

## I. Introduction

THERMAL detectors are essential devices for infrared (IR) spectroscopy and thermal imaging [1], [2], [3]. Due to the flat and broadband spectral response, these detectors are mostly used when measurements have to be performed over a wide spectral range from near-IR all the way to the far-IR regime. However, state-of-the-art uncooled thermal detectors' sensitivity is still several orders of magnitude below the fundamental detection limit, which is given by power fluctuations of thermal radiation from the detector and its background [1], [4].

Thermal detectors absorb the low-energy IR photons and measure the resulting photothermal heating. The temperature increase is usually measured electrically, for example, via a thermoelectric voltage, resistance change, or pyroelectric current. These electrical temperature sensing schemes are typically limited by thermal noise (Johnson noise) [1]. A mechanical IR-sensing concept was introduced in the late 1960s by Cary Instruments as a promising thermal detector that is not intrinsically limited by the thermal noise limit [5]. The principle of this concept is a macroscopic tensioned foil resonator that acts as the thermal-sensing element. Such macroscopic IR detectors have, to the best of our knowledge, never been successfully implemented at the time. It was only in 2011 when the successful fabrication and characterization of such a nanometer thin tensioned metal and silicon nitride (SiN) foil resonator elements for temperature sensing was first demonstrated [6]. Later in 2013, nanomechanical photothermal detector concepts based on tensioned SiN strings [7], [8] have been introduced. Recently, this concept has been developed further to be used as an IR detector based on a SiN drum featuring a broadband IR absorber thin film [9] and without a dedicated absorber [10], [11]. It has been shown that these drum resonators can reach an intrinsic sensitivity in the fW-regime [12]. It has further been shown that these structures enter the radiative heat-transfer regime for lateral drum sizes $>1$ mm [13], [14], [15].

Nanomechanical SiN resonators present a promising approach to creating thermal IR detectors that can reach

Manuscript received 13 August 2022; revised 11 October 2022; accepted 8 November 2022. Date of publication 28 November 2022; date of current version 12 January 2023. This work was supported in part by the European Research Council under the European Union's Horizon 2020 Research and Innovation Program under Grant 716087-PLASMECS and Grant 875518-NIRD and in part by Invisible-Light Labs GmbH. The authors acknowledge TU Wien Bibliothek for financial support through its Open Access Funding Programme. The associate editor coordinating the review of this article and approving it for publication was Prof. Tien-Kan Chung. *(Corresponding author: Silvan Schmid.)*

The authors are with the Institute of Sensor and Actuator Systems, Vienna University of Technology (TU Wien), 1040 Vienna, Austria (e-mail: markus.piller@tuwien.ac.at; johannes.hiesberger@tuwien.ac.at; elisabeth.wistrela@tuwien.ac.at; paolo.martini@tuwien.ac.at; niklas.luhmann@tuwien.ac.at; silvan.schmid@tuwien.ac.at).

Digital Object Identifier 10.1109/JSEN.2022.3223439

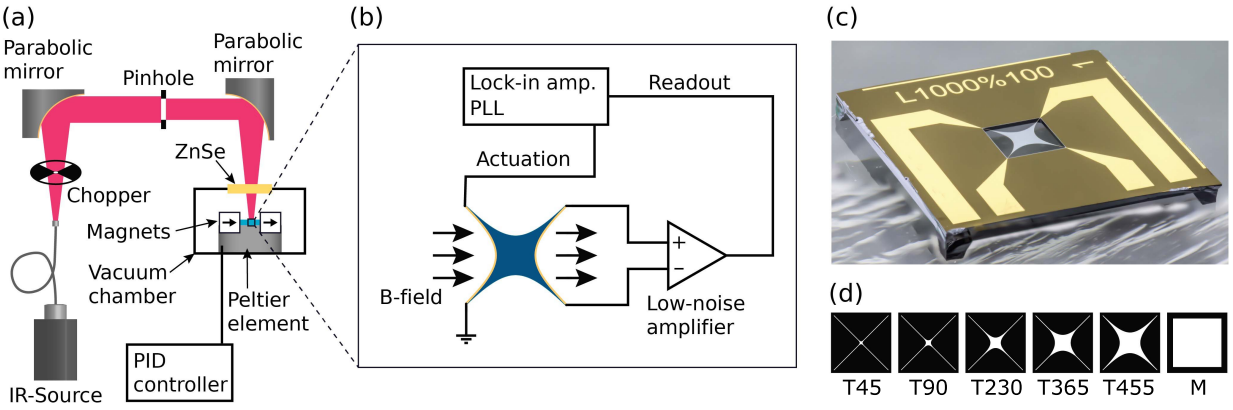


Fig. 1. (a) Schematic of the measurement setup. (b) Detailed schematic of the magnetomotive transduction scheme. (c) Microscope image of a trampoline resonator sample with gold electrodes (type T455). (d) Depiction of various trampoline resonator types used in this study. All resonators have a frame size of 1 × 1 mm and various detection areas reaching from the smallest T45 (45 × 45 $\mu$m) to the largest detection area at T455 (455 × 455 $\mu$m), and a drum resonator M with a size of 1000 × 1000 $\mu$m.

the long-anticipated photon noise limit. The same detector concept has been presented with graphene trampolines in the visible regime of the electromagnetic spectrum [16]. Other micro- and nanoelectromechanical (MEMS and NEMS) thermal detector concepts include piezoelectric resonators [17], [18], [19], torsional paddle resonators [20], [21], and polymer resonators [22].

Here, we investigated thermal IR detectors based on NEMS SiN trampoline resonators, which already proved exceptional properties in other fields [23], [24], [25], [26], [27]. Compared to drums, trampolines have enhanced thermal responsivity due to better thermal isolation of the central detection area [27].

We study and compare the performance of such trampoline-shaped IR detectors with various designs by means of their responsivity ($R$), noise-equivalent power (NEP), specific detectivity ($D^*$), and response time ($\tau_R$).

## II. Methods

### A. Experimental Setup

The experimental setup and the specific SiN trampolines with various detector area sizes that were studied are depicted in Fig. 1. The experimental setup comprises a broadband thermal IR light source (ArcLight IR form Arcoptix) with a spectral range from 1 to 25$\mu$m, an optical chopper (MC2000B and MC1F2 from Thorlabs, Inc.), two parabolic gold mirrors with a variable iris (pinhole) for intensity reduction, and a vacuum detector chamber. The chamber features a sample mount with two permanent magnets and a proportional–integral–derivative (PID)-controlled Peltier element to maintain a constant detector temperature of 20°C.

Before the characterization of our detector, the incident power of the IR radiation was measured with a reference detector (UM9B-BL-L-D0 from Gentec-Eo). The IR light was passing a fiber with a diameter of 900 $\mu$m. Using two parabolic mirrors with equal focal lengths, the optimal IR beam diameter on the detector corresponds to the fiber diameter, resulting in an average power after the zinc selenide (ZnSe) window of $P = 7\,\mu$W.

The NEMS trampoline detectors in this work are transduced by a magnetomotive scheme [28], [29], [30]. The necessary magnetic field is created by permanent magnets producing a field strength of $B \approx 0.6$ T. Two gold traces on the SiN trampolines are employed for separated actuation and readout of the nanomechanical motion. The trampoline's out-of-plane motion induces a voltage along the readout gold trace, which is connected to a differential low-noise voltage preamplifier (SR560 from Stanford Research Systems). A lock-in amplifier with a phase-locked loop module (HF2LI from Zurich Instruments) is used to create an oscillator based on the NEMS trampoline resonator, which was operated at the fundamental vibrational mode.

### B. Sample Fabrication

The trampoline resonators, shown in Fig. 1(c), are made of a low-stress silicon-rich SiN thin film with a thickness of 50 nm that was fabricated by low-pressure chemical vapor deposition. The 5-$\mu$m wide trampoline tethers are supported by a silicon frame with a thickness of 380 $\mu$m. All chips are 5 × 5 mm large with a frame size of 1 × 1 mm. The 1-$\mu$m-wide gold electrodes with a thickness of 190and 10nm chromium adhesion layer beneath were added by thermal evaporation (Balzers BAK-550).

The fabrication process is outlined in Fig. 2. The fabrication of the SiN trampolines (a) starts with the deposition of gold (Au) electrodes on the SiN layer. For this purpose, a silicon (Si) wafer with double-sided SiN layers (b) is spin-coated with photoresist (c) on one side and structured in a photolithography step (d). The gold electrodes are then deposited via thermal evaporation (e). The excess gold and the photoresist are removed with a standard lift-off process (f). A new photoresist layer is spin-coated on the top and bottom of the wafer (g) to structure the top for the trampoline and protect the bottom (h). The SiN trampoline shape is structured by reactive ion etching (i) and has to be released from the Si. Therefore, a square window is patterned in the backside resist (j), and SiN is removed through reactive ion etching (k). As one of the final steps, the Si is etched in KOH to release the SiN trampoline (l).

In the final step [Fig. 2(m)], a platinum (Pt) thin film is deposited via thermal evaporation on the backside. This ultrathin Pt film acts as an impedance-matched absorber with

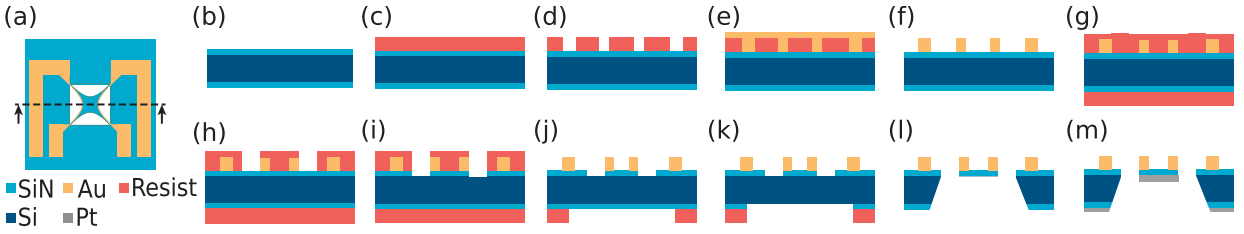


Fig. 2. Sample fabrication steps for SiN trampoline resonators with gold electrodes. (a) Schematic of a trampoline with a color-coded legend for the different materials. (b)–(m) Dashed line indicates the cross section used to explain the fabrication steps.

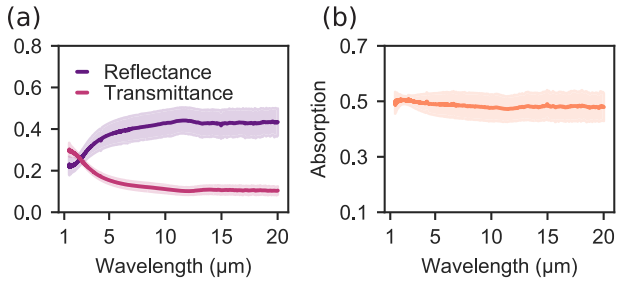


Fig. 3. (a) Measured transmittance and reflectance spectra for a 50-nm SiN drum with a 5-nm platinum thin film and (b) corresponding absorption spectrum.

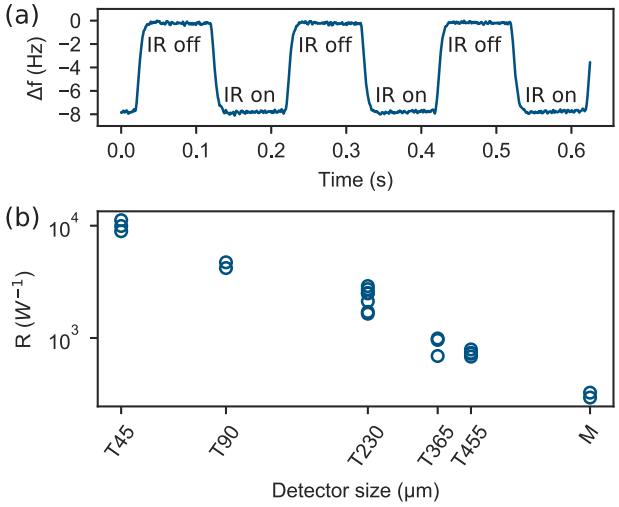


Fig. 4. IR characterization measurements for responsivity. (a) PLL measured resonance frequency for a chopped IR light at 5 Hz exemplary for a trampoline T45. (b) Relative responsivity obtained for different detector sizes of trampolines. Each data point corresponds to a measurement of an individual sample of the denoted size depicted in Fig. 1(d).

a flat spectral response for a wavelength range from 1 to 25 $\mu$m, as shown in Fig. 3. This absorber is made of a Pt thin film with a thickness of 5 nm. Such an impedance-matched absorber provides optimal absorption of 50% over the whole spectral range from 1 to 25 $\mu$m [31], [32], [33], which was confirmed by spectral measurements via Fourier-transform IR spectroscopy (Bruker Tensor 27) equipped with a transmittance and reflectance unit (Bruker A510/Q-T). Fig. 3(a) shows the obtained transmittance $T$ and reflectance $R$ spectra from which the absorption $\alpha$ readily can be calculated as $\alpha = 1-R-T$, as shown in Fig. 3(b).

## III. Results and Discussion

The detection mechanism is based on photothermal detuning of the resonators' resonance frequency. The incident light causes a change in the temperature of the resonator and a thermal expansion leading to a reduction of the tensile stress [7], [8], [9], [34]. Hence, the responsivity of such an NEMS detector with a detector area $A$ is given by the relative frequency change $\delta f = \Delta f/f_0$ per power of IR light irradiated over the detector area

$$R = \frac{\delta f}{P_{\text{abs}}}. \tag{1}$$

The absorbed power $P_{\text{abs}}$ is the integrated power over the area of the Gaussian beam profile. Fig. 4(a) shows a typical frequency measurement where the IR light has been turned on and off, at a measured fundamental frequency $f_0 = 24.5\,\text{kHz}$. From such time-resolved response measurements, the responsivity of each NEMS detector was derived, as shown in Fig. 4(b). The measured responsivities steadily increase for smaller trampoline detector sizes. Since the frame size is fixed for all detectors to a size of 1 mm, the tether length of the trampolines linearly scales with the detector area. The tethers become longer for a smaller detector area, which causes improved thermal isolation. The observed enhanced responsivity of trampolines with small detector areas can hence be attributed to the increased tether length. The responsivity in the conductive heat-transfer regime of the trampolines can be approximated by two crossing strings of length $L$ [30], [34]

$$R = -\frac{\alpha E L}{32\kappa\sigma h w} \tag{2}$$

with the thermal expansion coefficient $\alpha$, Young's modulus $E$, thermal conductivity $\kappa$, tensile stress $\sigma$, and string cross-section area $h \times w$. $R$ is proportional to $L$ resulting in a linear decrease of $R$ with detector area, as it is clearly observable in Fig. 4(b), in particular, for the smallest trampolines. The measured maximum responsivity of $R = 11\,000\ \text{W}^{-1}$ is more than one order of magnitude below the values obtained with plain SiN drums and external interferometric readout [12]. According to (2), the reason is the Au electrodes that pass over the drum and significantly increase the thermal conductivity. An external interferometer is not a practical readout method, hence here we use an integrated electronic readout that comes with a tradeoff in responsivity.

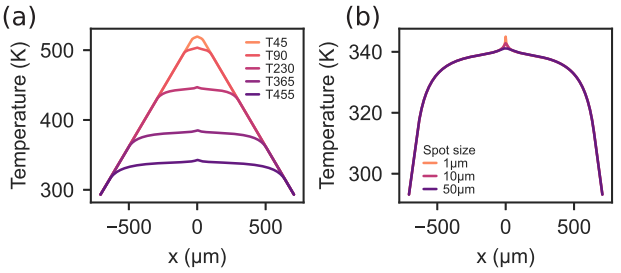


Fig. 5. Finite-element simulations of the temperature profile across SiN trampolines for $P_{abs} = §1$ mw considering conductive heat transfer only. (a) Temperature profile for different sizes of trampolines for an IR spot size of 10 $\mu$m. (b) Temperature profile for the very center part of a T455 trampoline for different IR spot sizes.

Fig. 5(a) shows temperature profiles for different trampoline types at constant absorbed power. The results were obtained by finite-element method simulations. The simulations show that the improvement in responsivity with a smaller detection area can be explained by the correspondingly enhanced temperature profile. As Fig. 5(a) shows, the resonator temperature is inversely related to the detection area.

The effect of different IR spot sizes on the temperature profile is shown in Fig. 5(b) for a T455 trampoline. A small spot size causes only an insignificant local temperature peak, which does not affect the overall temperature profile. This shows that the spot size does not have a significant effect on the responsivity, as long as it is smaller than the detection area.

Next, the sensitivity is determined in terms of the NEP. The NEP of a NEMS detector directly scales with the frequency resolution, which was determined through the respective Allan deviation $\sigma_{AD}$ for a given integration time $\tau$

$$\text{NEP} = \frac{\sigma_{AD} \cdot \sqrt{\tau}}{R}. \tag{3}$$

The Allan deviation was calculated from frequency recordings over 1 min of each NEMS resonator. An example of the Allan deviation for a T45 sample is shown in Fig. 6(a). The marker in Fig. 6(a) indicates the integration time $\tau = 40$ ms that has been selected to calculate the resulting NEP. At this integration time, the slope of the measured Allan deviation curve is proportional to $1/\sqrt{\tau}$, resulting in a minimal NEP (3).

Fig. 6(b) presents the measured NEPs of all NEMS trampoline resonators. The NEP improves for trampolines with small detection areas, according to the enhanced responsivity of these structures due to the longer tethers. Compared to the drum resonators (M), the NEP of the trampolines was improved by up to two orders of magnitude. The smallest trampolines showed an NEP of 7 pW/$\sqrt{\text{Hz}}$.

Fig. 6(c) presents the obtained specific detectivity $D^* = \sqrt{A}/\text{NEP}$, which normalizes the sensitivity of a detector with its detection area $A$. $D^*$ is typically used to compare quantum detectors for which noise power is directly proportional to detector size. Noise in thermal detectors does not necessarily follow this trend [35]. However, the trampolines' responsivity is inversely proportional to the detector size as discussed above. Hence, the measured specific detectivity values are

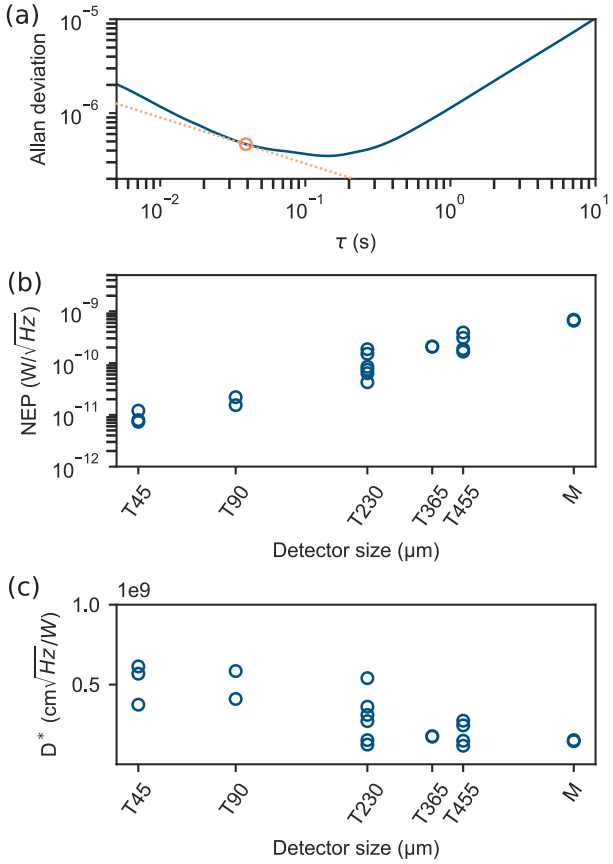


Fig. 6. (a) Measured Allan deviation and marked value used for the sensitivity, exemplary for a trampoline T45. The dashed line represents a slope proportional to $1/\sqrt{\tau}$. (b) NEP and (c) corresponding specific detectivity obtained for various sample sizes, where each data point corresponds to a measured value of an individual sample.

constant to a good approximation, in particular, for the smallest trampolines with the longest tethers.

Fig. 7 shows the measured response times, which were obtained from the 90/10 method [36] by calculating the rise time from step transition and relating it to a first-order low-pass filter model. The trampolines with the smallest detector size show an improved behavior toward faster response times. The response time of a thermal detector $\tau_R = C/G$ is given by the ratio of heat capacity $C$ to heat conductance $G$. When reducing the detector size, both the heat capacity and conductance decrease. Because $C$ scales with the detector area and $G$ with the tether length, the response times get faster for trampolines with smaller detector sizes. The smallest trampolines performed best with response times of 4 ms.

Fig. 8 shows a finite-element method simulation of the in-plane stress along the diagonal of a trampoline structure T230, with an initial stress of 150 MPa. It shows an increase in tensile stress in the tethers that hold the detection area which is inherent to the trampoline design. The maximum stress in the tethers of $\sigma = 185$ MPa is more than one order of magnitude below the yield strength of SiN ($\sigma_{\text{yield}} \approx 6$ GPa [37]). We have not observed any failure of fatigue of SiN trampoline resonators since we have been fabricating these over the last three years [26], [27]. At operation in the linear

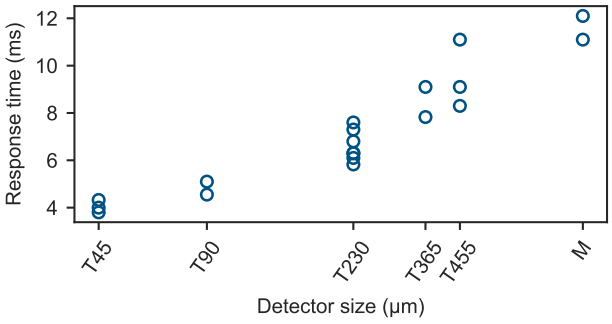


Fig. 7. Comparison of the thermal response time analysis between different trampolines and the drum resonator.

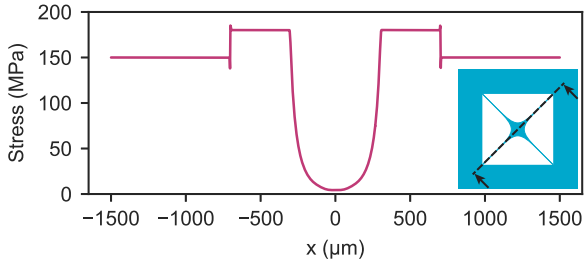


Fig. 8. Stress profile calculated with the finite-element method for a trampoline structure T230 with an initial stress of 150 MPa.

regime with maximal amplitudes of 10 nm no material fatigue has been observed.

## IV. Conclusion

We demonstrate trampoline structures made of SiN as enhanced NEMS-based IR detectors. Compared to other SiN [9], [11], [38] or piezoelectric [17], [18] nanomechanical resonators as IR detectors with sensitivities in the range of hundreds of $\mathrm{pW}/\sqrt{\mathrm{Hz}}$, we could improve the NEP by two orders of magnitude with a minimum measured value of $7\ \mathrm{pW}/\sqrt{\mathrm{Hz}}$. Furthermore, we could also improve the response time by a factor of 3 compared to SiN drum detectors [9]. The smaller the detector area, the longer become the tethers, which results in enhanced sensitivity. This clearly shows the potential of NEMS-based thermal detectors. However, one of the challenges is still to convert the improved IR detection methods into application-oriented sensors with the same performance. We have taken a step in this direction with this work by designing NEMS SiN trampoline detectors with a broadband absorber and integrated electronic readout.

Larger detector areas can readily be obtained in a future design by increasing the frame dimensions. With the current NEP, a detector area of $A = 1\times1\ \mathrm{mm}$ would result in the theoretical photon noise limit of $D^* \approx 2\times10^{10}\ \mathrm{cm}\sqrt{\mathrm{Hz}}/\mathrm{W}$ [1]. Finally, the responsivity can be improved by using a transduction principle that does not require metal leads that pass over the trampoline structure and hence is less deteriorating to the responsivity. Such NEMS resonators are promising thermal IR detector schemes with the potential to reach the ultimate photon noise sensitivity limit.

## Acknowledgment

The authors wish to thank Sophia Ewert, Patrick Meyer, and Michael Buchholz for their support with the sample fabrication as well as Hendrik Kähler and Robert G. West for many fruitful discussions. They would also like to thank Georg Pfusterschmied for his support.

## References

[1] A. Rogalski, *Infrared and Terahertz Detectors*, 3rd ed. Boca Raton, FL, UASA: CRC Press, Jan. 2019, doi: 10.1201/b21951.
[2] P. G. Datskos and N. V. Lavrik, "Detectors—Figures of merit," in *Encyclopedia of Optical Engineering*, vol. 349, 2003, p. 100.
[3] J. T. Skidmore, J. Gildemeister, A. T. Lee, M. J. Myers, and P. L. Richards, "Superconducting bolometer for far-infrared Fourier transform spectroscopy," *Appl. Phys. Lett.*, vol. 82, no. 3, pp. 469–471, Jan. 2003.
[4] P. W. Kruse, "Can the 300-K radiating background noise limit be attained by uncooled thermal imagers?" in *Proc. SPIE*, Aug. 2004, pp. 437–446.
[5] H. H. Cary, "Infrared radiation detector employing tensioned foil to receive radiation," U.S. Patent US3 457 412A, vol. 7, 1969.
[6] T. Larsen et al., "Ultrasensitive string-based temperature sensors," *Appl. Phys. Lett.*, vol. 98, no. 12, Mar. 2011, Art. no. 121901. [Online]. Available: http://ieeexplore.ieee.org/xpls/abs_all.jsp?arnumber=5738575
[7] S. Yamada, S. Schmid, T. Larsen, O. Hansen, and A. Boisen, "Photothermal infrared spectroscopy of airborne samples with mechanical string resonators," *Anal. Chem.*, vol. 85, no. 21, pp. 10531–10535, Nov. 2013.
[8] T. Larsen, S. Schmid, and A. Boisen, "Micro string resonators as temperature sensors," in *Proc. AIP Conf.*, 2013, pp. 931–936.
[9] M. Piller, N. Luhmann, M.-H. Chien, and S. Schmid, "Nanoelectromechanical infrared detector," in *Proc. SPIE*, Sep. 2019, pp. 9–15, doi: 10.1117/12.2528416.
[10] C. Zhang, M. Giroux, T. A. Nour, and R. St-Gelais, "Thermal radiation sensing using high mechanical Q-factor silicon nitride membranes," in *Proc. IEEE SENSORS*, Oct. 2019, pp. 1–4.
[11] N. Snell, C. Zhang, G. Mu, and R. St-Gelais, "Nanowatt thermal radiation sensing using silicon nitride nanomechanical resonators," in *Proc. Photon. North (PN)*, May 2020, P. 1.
[12] M.-H. Chien, M. Brameshuber, B. K. Rossboth, G. J. Schütz, and S. Schmid, "Single-molecule optical absorption imaging by nanomechanical photothermal sensing," *Proc. Nat. Acad. Sci. USA*, vol. 115, no. 44, pp. 11150–11155, Oct. 2018. [Online]. Available: http://www.pnas.org/lookup/doi/10.1073/pnas.1804174115
[13] M. Piller et al., "Thermal radiation dominated heat transfer in nanomechanical silicon nitride drum resonators," *Appl. Phys. Lett.*, vol. 117, no. 3, Jul. 2020, Art. no. 034101.
[14] P. Sadeghi, M. Tanzer, N. Luhmann, M. Piller, M.-H. Chien, and S. Schmid, "Thermal transport and frequency response of localized modes on low-stress nanomechanical silicon nitride drums featuring a phononic-band-gap structure," *Phys. Rev. A, Gen. Phys. Appl.*, vol. 14, no. 2, Aug. 2020, Art. no. 024068.
[15] C. Zhang, M. Giroux, T. A. Nour, and R. St-Gelais, "Radiative heat transfer in freestanding silicon nitride membranes," *Phys. Rev. A, Gen. Phys. Appl.*, vol. 14, no. 2, Aug. 2020, Art. no. 024072.
[16] A. Blaikie, D. Miller, and B. J. Alemán, "A fast and sensitive room-temperature graphene nanomechanical bolometer," *Nature Commun.*, vol. 10, no. 1, p. 4726, Dec. 2019.
[17] Z. Qian, V. Rajaram, S. Kang, and M. Rinaldi, "High figure-of-merit NEMS thermal detectors based on 50-nm thick AlN nano-plate resonators," *Appl. Phys. Lett.*, vol. 115, no. 26, Dec. 2019, Art. no. 261102.
[18] Y. Zhang, S. Hosono, N. Nagai, S.-H. Song, and K. Hirakawa, "Fast and sensitive bolometric terahertz detection at room temperature through thermomechanical transduction," *J. Appl. Phys.*, vol. 125, no. 15, Apr. 2019, Art. no. 151602.
[19] Y. Hui, S. Kang, Z. Qian, and M. Rinaldi, "Uncooled infrared detector based on an aluminum nitride piezoelectric fishnet metasurface," *J. Microelectromech. Syst.*, vol. 30, no. 1, pp. 165–172, Feb. 2021.
[20] X. C. Zhang, E. B. Myers, J. E. Sader, and M. L. Roukes, "Nanomechanical torsional resonators for frequency-shift infrared thermal sensing," *Nano Lett.*, vol. 13, no. 4, pp. 1528–1534, Apr. 2013.
[21] L. Laurent, J.-J. Yon, J.-S. Moulet, M. Roukes, and L. Duraffourg, "12–$\mu$m-pitch electromechanical resonator for thermal sensing," *Phys. Rev. A, Gen. Phys. Appl.*, vol. 9, no. 2, Feb. 2018, Art. no. 024016, doi: 10.1103/PhysRevApplied.9.024016.

[22] U. Adiyan, T. Larsen, J. J. Zárate, L. G. Villanueva, and H. Shea, "Shape memory polymer resonators as highly sensitive uncooled infrared detectors," *Nature Commun.*, vol. 10, no. 1, pp. 1–9, Dec. 2019.
[23] R. A. Norte, J. P. Moura, and S. Gröblacher, "Mechanical resonators for quantum optomechanics experiments at room temperature," *Phys. Rev. Lett.*, vol. 116, no. 14, Apr. 2016, Art. no. 147202, doi: 10.1103/PhysRevLett.116.147202.
[24] C. Reinhardt, T. Müller, A. Bourassa, and J. C. Sankey, "Ultralow-noise SiN trampoline resonators for sensing and optomechanics," *Phys. Rev. X*, vol. 6, no. 2, Apr. 2016, Art. no. 021001.
[25] R. Fischer et al., "Spin detection with a micromechanical trampoline: Towards magnetic resonance microscopy harnessing cavity optomechanics," *New J. Phys.*, vol. 21, no. 4, Apr. 2019, Art. no. 043049.
[26] M.-H. Chien and S. Schmid, "Nanoelectromechanical photothermal polarization microscopy with 3 Å localization precision," *J. Appl. Phys.*, vol. 128, no. 13, Oct. 2020, Art. no. 134501.
[27] M.-H. Chien, J. Steurer, P. Sadeghi, N. Cazier, and S. Schmid, "Nanoelectromechanical position-sensitive detector with picometer resolution," *ACS Photon.*, vol. 7, no. 8, pp. 2197–2203, Aug. 2020.
[28] W. J. Venstra, H. J. R. Westra, K. B. Gavan, and H. S. J. van der Zant, "Magnetomotive drive and detection of clamped-clamped mechanical resonators in water," *Appl. Phys. Lett.*, vol. 95, no. 26, Dec. 2009, Art. no. 263103.
[29] T. Kouh, M. S. Hanay, and K. L. Ekinci, "Nanomechanical motion transducers for miniaturized mechanical systems," *Micromachines*, vol. 8, no. 4, p. 108, 2017.
[30] S. Schmid, L. G. Villanueva, and M. L. Roukes, *Fundamentals Nanomechanical Resonators*. Berlin, Germany: Springer, 2016, doi: 10.1007/978-3-319-28691-4.
[31] C. Hilsum, "Infrared absorption of thin metal films," *J. Opt. Soc. Amer.*, vol. 44, no. 3, p. 188, 1954.
[32] N. Luhmann et al., "Ultrathin 2 nm gold as impedance-matched absorber for infrared light," *Nature Commun.*, vol. 11, no. 1, p. 2161, Dec. 2020.
[33] T. Kenny, "Chapter 8 tunneling infrared sensors," in *Uncooled Infrared Imaging Arrays and Systems* (Semiconductors and Semimetals), vol. 47, P. W. Kruse and D. D. Skatrud, Eds. Amsterdam, The Netherlands: Elsevier, 1997, pp. 227–267. [Online]. Available: https://www.sciencedirect.com/science/article/pii/S0080878408626940
[34] S. Schmid, K. Wu, P. E. Larsen, T. Rindzevicius, and A. Boisen, "Low-power photothermal probing of single plasmonic nanostructures with nanomechanical string resonators," *Nano Lett.*, vol. 14, pp. 2318–2321, Apr. 2014. [Online]. Available: http://www.ncbi.nlm.nih.gov/pubmed/24697597
[35] P. G. Datskos and N. V. Lavrik, "Detectors—Figures of merit," in *Encyclopedia in Optical Engineering*, R. Driggers, Ed. New York, NY, USA: Marcel Dekker, 2003, pp. 349–357.
[36] L. Duraffourg, L. Laurent, J.-S. Moulet, J. Arcamone, and J.-J. Yon, "Array of resonant electromechanical nanosystems: A technological breakthrough for uncooled infrared imaging," *Micromachines*, vol. 9, no. 8, p. 401, Aug. 2018. [Online]. Available: http://www.mdpi.com/2072-666X/9/8/401
[37] A. H. Ghadimi et al., "Elastic strain engineering for ultralow mechanical dissipation," *Science*, vol. 360, pp. 764–768, May 2018.
[38] L. Vicarelli, A. Tredicucci, and A. Pitanti, "Micromechanical bolometers for subterahertz detection at room temperature," *ACS Photon.*, vol. 9, no. 2, pp. 360–367, Feb. 2022.

**Markus Piller** received the degree in electrical engineering and embedded systems and the master's degree from the Vienna University of Technology (TU Wien), Vienna, Austria, in 2018 and 2018, respectively. He is currently pursuing the Ph.D. degree with CERN, Geneva, Switzerland.

He continued his research at the Micro and Nanosensors Research Group of Prof. Silvan Schmid, TU Wien. He is currently a Researcher at CERN focused on analog microelectronics for fast-timing detectors.

**Johannes Hiesberger** received the B.Sc. degree in electrical engineering from the Vienna University of Technology (TU Wien), Vienna, Austria, in 2021, where he is currently pursuing the master's degree in embedded systems.

He was with the Research Group of Prof. Silvan Schmid, TU Wien.

**Elisabeth Wistrela** received the Ph.D. degree in microelectronics from the Vienna University of Technology (TU Wien), Vienna, Austria, in 2020. She performed her Ph.D. thesis at the Institute of Sensor and Actuator Systems, Vienna, Microsystems Technology, where she investigated the impact of doping on piezoelectric aluminum nitride thin films.

**Paolo Martini** is currently pursuing the Ph.D. degree with Prof. Silvan Schimd's Research Group, Vienna University of Technology (TU Wien), Vienna, Austria, focusing his research on room-temperature IR sensing.

After his graduation from the Polytechnic University of Turin, Turin, Italy, in 2019, he joined Prof. Silvan Schimd's Research Group, TU Wien. He is a Biomedical Engineer specialized in Bio-Nanotechnologies.

**Niklas Luhmann** received the master's degree in physics from the University of Konstanz, Konstanz, Germany, in 2017. He is currently pursuing the Ph.D. degree with the Micro- and Nanosensor Group of Prof. Silvan Schmid, Vienna University of Technology (TU Wien), Vienna, Austria.

During his master's degree, he joined the Micro- and Nanosensor Group of Prof. Silvan Schmid, TU Wien, and specialized in nanomechanical systems. He has an early focus set on applied sensor applications at the Centro Atomico Bariloche, Bariloche, Argentina. He is the Co-Founder at Invisible-Light Labs GmbH, Vienna, focusing his research on nanomechanical infrared spectroscopy and commercialization of the technology.

**Silvan Schmid** received the degree in mechanical engineering and the Ph.D. degree in micro- and nanosystem technology from Eidgenössische Technische Hochschule (ETH) Zurich, Zürich, Switzerland, in 2004 and 2009, respectively.

From 2009 to 2016, he worked at the Institute of Micro- and Nanotechnology (DTU Nanotech), Technical University of Denmark, Kongens Lyngby, Denmark. In 2016, he was appointed as a Full Professor at the Institute of Sensor and Actuator Systems, Vienna University of Technology (TU Wien), Vienna, Austria, where he currently leads the Research Unit for Micro- and Nanosensors. In 2019, he co-founded the startup Invisible-Light Labs GmbH, Vienna. In 2021, he was appointed as the Dean of Academic Affairs for the Faculty of Electrical Engineering and Information Technology, TU Wien.

Dr. Schmid was awarded the ETH Medal for his Ph.D. degree. He also received the Villum's Young Investigator Award from DTU Nanotech, Technical University of Denmark. In 2016, he also received an European Research Council (ERC) Starting Grant followed by an ERC Proof of Concept Grant in 2019.